Strength of Materials, Vol. 43, No. 2, March, 2011

A GENERALIZED GRAIN-SIZE DEPENDENCE OF THE FATIGUE LIMIT

O. M. Herasymchuk

UDC 539.4;669.295

A generalized model is developed for calculating the fatigue limit of the material based on the data on its microstructure. The experimental results of fatigue and cyclic fracture toughness tests and the data on the analysis of the microstructure of two-phase ($\alpha + \beta$) titanium VT3-1 alloy with a different microstructure (globular, bimodal and fine lamellar microstructure) have shown that the dependence of the fatigue limit on the structural parameter, which is responsible for the material fatigue strength, has a nonlinear S-like nature. The formula for calculating the fatigue limit is justified by the data on the microstructural parameters and by the results of static tensile tests of the material, with a fair agreement obtained between the calculated and experimental results. The model has been validated for materials with another type of the crystal lattice [steel containing 0.16% C with a body-centered cubic lattice (bcc) and brass 70/30 with a face-centered cubic lattice (fcc)] and has shown a satisfactory agreement between the experimental and calculation results.

Keywords: fatigue, fatigue limit, structural parameter, crystal lattice.

Introduction. In view of the current widespread use of advanced structural materials in mechanical engineering and also the extension of the notion about the ultimate potential of traditionally used alloys due to the optimization of their processing, the need to determine the characteristics of resistance to fatigue fracture increases dramatically. It should be noted that the traditional correlation relationships that connect the characteristics of cyclic strength with those of static strength and microstructure cannot be used for novel advanced materials and new processes for manufacturing components as being untested and such that do not provide the desired accuracy for determining the fatigue strength characteristics. The carrying out of experimental studies on the fatigue strength characteristics of new alloys in order to optimize their manufacturing process with the methods specified in current standards results in extremely high consumption of material resources and time. In many cases, an important point is that the required data on the material strength under cyclic loading are to be obtained in the shortest possible time (for instance, to verify the correctness of the engineering design or technology decision made), and the data from traditional long-term tests obtained untimely quite often lose their value.

One of the most important parameters of the material microstructure which is currently associated with the fatigue limit is the grain size, d. Already the pioneering studies on the effect of the grain size on the fatigue fracture resistance started as early as the 30s of the last century have revealed that the fatigue limit increases with a decrease in the grain size. However, in a number of papers it was noted that a finer microstructure does not necessarily result in the lifetime change. The linear relationship between the yield stress and the parameter of microstructure $1/\sqrt{d}$ derived in [1, 2] and a similar relationship for the fatigue limit derived in [3] are currently used by numerous authors as empirical relationships. However, these relationships describe the grain-size dependence of the fatigue limit only in the range limited for each material and, as will be shown later, are not always quite correct.

On the other hand, i.e., from the linear fracture mechanics standpoint, the fatigue limit can be considered as the maximum stress amplitude at which the fatigue crack, appeared in the material as a result of the cyclic loading, has stopped and no longer propagates. Based on these standpoints, numerous authors [4, 5] arrived at the representation of the fatigue limit $\Delta\sigma_R$ as

Pisarenko Institute of Problems of Strength, National Academy of Sciences of Ukraine, Kyiv, Ukraine. Translated from Problemy Prochnosti, No. 2, pp. 128 – 144, March – April, 2011. Original article submitted October 19, 2009.

$$\Delta\sigma_R = \frac{\Delta K_{th}}{Y\sqrt{l_0}}, \tag{1}$$

where ΔK_{th} is the threshold value of the stress intensity factor (SIF) range, Y is the function that takes into account the crack and body geometry and conditions of loading, and l_0 is the so-called "critical crack length" that corresponds to the fatigue limit.

A linear dependence of l_0 on the mean grain size d was derived in [6] for various alloys and steels:

$$l_0 = \eta d, \tag{2}$$

where $\eta > 1$ is the proportionality factor. However, formula (1) in this form cannot be applied to predict the material fatigue limit since l_0 is unknown.

The purpose of this work is to develop a model for calculating the fatigue limit of the material based on the data on its microstructure and from the results of static tensile tests that would allow the prediction of the fatigue limit at a fully-reversed loading cycle, σ_{-1}, in the whole range of sizes of the microstructural element responsible for the fatigue strength of the studied material. It should be noted that the term "microstructural element size" is used here as a general one, since it includes both a linear grain size for single-phase materials and the size that defines the diameter of α-globules, the thickness of α-lamellas, the thickness of the intergranular α-spacing, etc., for example for two-phase titanium alloys.

Materials and Experimental Procedures. The object of the experimental investigation was a two-phase ($\alpha + \beta$) titanium VT3-1 alloy [7, 8] that was studied in the form of an initial bar and billets after different modes of thermomechanical treatment.

The starting bars were subjected to preliminary quenching (1323 K, holding in a furnace for 0.5 h), in order to attain the dispersed α-state and to eliminate the texture formed during the manufacture of bars. After quenching, the bars were rolled using a two-high rolling mill under isothermal conditions at temperatures of 1073 to 1223 K (heating in laboratory resistance furnaces) with a total reduction of 60 to 70% (a reduction of 10 to 12% per one pass). The final recrystallization annealing (at 1073 K, holding for 5 h) was carried out in a vacuum furnace at a residual pressure no higher than 10 Pa. One batch of billets was subjected to the "rapid heat treatment" by electrical contact heating using current of mains frequency in accordance with the data in [9, 10], in order to obtain a special fine-grained β-transformed (FGBT) microstructure. After attaining the predetermined heating temperature, the cooling was carried out in air which made it possible to reach the alloy state exhibiting the most balanced characteristics of the mechanical properties, rather than the state with the highest strength only. Aging performed under standard conditions [9] was the finishing stage to obtain a stable phase and structural state. Moreover, the microstructural state of VT3-1 alloy was obtained that simulates the microstructure after appropriate conditions of thermomechanical treatment used in industrial practice for this alloy in the manufacture of semi-finished products for aircraft engine fan blades. In total, 7 types of microstructural states of VT3-1 alloy were investigated, 6 types with globular and bimodal microstructures, and one type with a FGBT fine lamellar microstructure.

The microstructure of the alloys was studied using the methods of optical and electronic microscopy, and the quantitative characteristics of certain microstructural components were obtained using the software Image Pro. The microstructures of the materials under investigation are shown in Fig. 1.

The fatigue tests were performed under normal conditions on smooth specimens with a working section of 5×5 mm in the plane cantilever bending at fully-reversed cyclic loading using an electrodynamic vibration-testing machine according to the procedures described in detail in [7, 8]. The 1% drop in the resonant frequency of the specimen vibrations that corresponds to the formation of a semi-elliptical surface crack of a depth of about 10% of the specimen section thickness was considered as the fatigue fracture criterion. After recording the number of cycles N to fatigue fracture, the specimens were run to final fracture, i.e., the separation into two pieces, in order to investigate fracture surfaces using a scanning electron microscope.

The results of microstructural investigations are given in Table 1 together with the characteristics of the mechanical properties in static tension: the offset yield strength $\sigma_{0.2}$, the ultimate strength σ_u, the relative

TABLE 1. Microstructure Characterization and Mechanical Properties of VT3-1 Alloy

No. of the microstructure	Microstructure type	Texture characterization	Average size d of the microstructural element		$\sigma_{0.2}$, MPa	σ_u, MPa	δ, %	ψ, %
			Diameter of α-globules, μm	Thickness of α-lamellas, μm				
1	FGBT	Unpronounced	–	0.4	1030	1544	3	11
2	Bimodal	BP texture, strong	1.8	0.2	1011	1070	16	30
3	ditto	Weakly pronounced	2.0	0.1	1065	1114	15	48
4	ditto	BP texture, strong	2.5	1.5	1027	1084	15	25
5	ditto	ditto	3.0	0.7	1009	1069	15	22
6	Globular	Weakly pronounced	4.0	–	1100	1210	13	20
7	ditto	ditto	10.0	–	998	1026	9	17

* Basal-and-prismatic texture (BP).

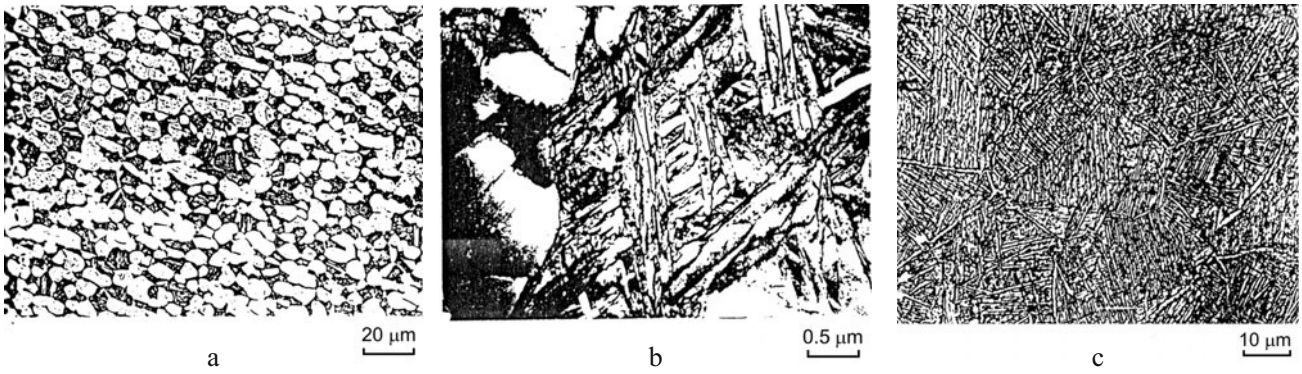

a b c

Fig. 1. A bimodal (a), (b) and a FGBT microstructure (c) of VT3-1 alloy.

elongation δ, the reduction of cross-sectional area ψ. The fatigue test results are given in Fig. 2, and their detailed analysis made earlier [7, 8].

Development of the Model for Predicting the Fatigue Limit. In [13], using titanium VT3-1 alloy with a globular and bimodal microstructures as an example, the dependence of the fatigue limit σ_{-1} on the grain size d (i.e., the average diameter of α-globules) was represented in the form

$$\sigma_{-1} = \frac{\Delta K_{th\,eff}}{Y\sqrt{d}}, \tag{3}$$

where σ_{-1} is the fatigue limit under fully reversed cyclic bending loading and $\Delta K_{th\,eff}$ is the threshold value of the effective SIF range for long cracks, i.e., for cracks of the length (depth) $l \geq l_0$.

The calculation of σ_{-1} by the above formula (3) has shown good agreement with the experimental results for six sizes of α-globules (Tables 1 and 2).

It should be noted that the value of $\Delta K_{th\,eff}$ in Eq. (3) was calculated by the formula derived in [11] in the investigation of a wide range of metals of different grades,

$$\Delta K_{th\,eff} \approx 1.6 \cdot 10^{-5} E \ [\text{MPa}\sqrt{\text{m}}], \tag{4}$$

where E is the elastic modulus, MPa.

In [8], it was also shown that the calculation by formula (4) for alloy VT3-1 under study (with $E = 127.5$ GPa and $\Delta K_{th\,eff} = 2.04$ MPa$\sqrt{\text{m}}$) is in good agreement with the experimental value of $\Delta K_{th\,eff}^{exp} = 2.05$ MPa$\sqrt{\text{m}}$ for the studied microstructural states of VT3-1 alloy. In the general case of bending, the function Y [12] takes the form:

TABLE 2. Comparison between the Calculated σ_{-1}^{calc} calc and Experimental σ_{-1}^{exp} Results for VT3-1 Alloy

No. of the microstructure	Microstructure type	d, μm	σ_{-1}^{exp}, MPa	σ_{-1}^{calc}, MPa	Δ*, %
1	FGBT	0.4	800	1621	+ 103.0
2	Bimodal	1.8	750	764	+ 1.9
3	Bimodal	2.0	700	725	+ 3.6
4	Bimodal	2.5	650	649	− 0.2
5	Bimodal	3.0	600	593	− 1.3
6	Globular	4.0	520	513	− 1.4
7	Globular	1.,0	350	324	− 7.4

* The relative error $\Delta = [(\sigma_{-1}^{calc} - \sigma_{-1}^{exp}) / \sigma_{-1}^{exp}] \cdot 100\%$.

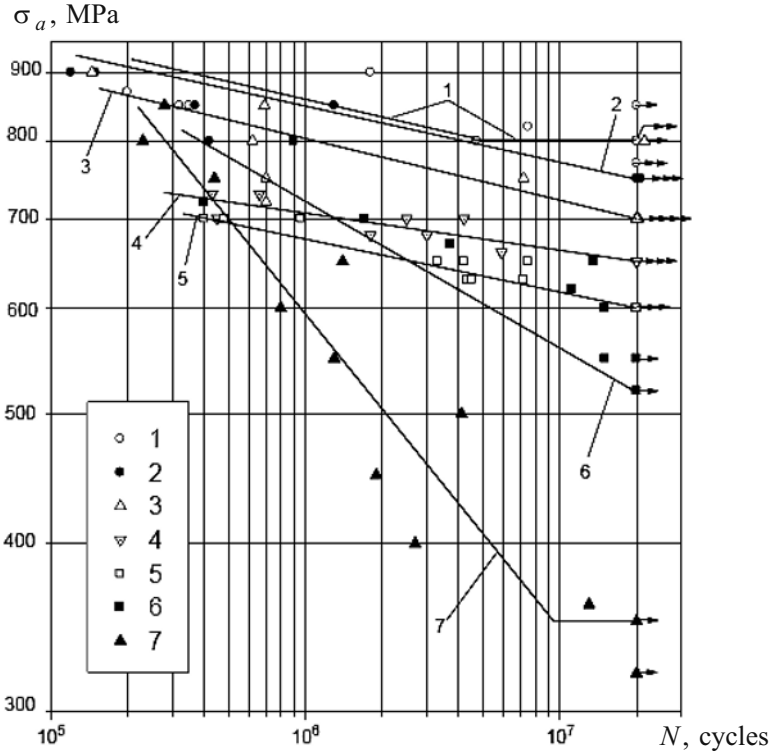

Fig. 2. Fatigue curves for VT3-1 alloy: (*1–7*) correspond to the microstructure type (Tables 1–4).

$$Y = 1.99 - 2.47(l/b) + 12.97(l/b)^2 - 23.18(l/b)^3 + \ldots, \quad (5)$$

where l is the crack depth and b is the specimen thickness in the working section. Since the crack depth $l = l_0$ is negligibly small as compared to the specimen thickness, the value of $Y = 1.99$ was taken for the calculation, with the other terms of the series being neglected.

The analysis of the specimen fracture surfaces [8] shows that for VT3-1 alloy with a globular and bimodal microstructure, the crack nucleation occurs in the globular α-phase, i.e., it was the α-globules in these structures that are responsible for the fatigue strength of VT3-1 alloy. In contrast to it, in the material with a FGBT lamellar microstructure, the fatigue crack nucleation was initiated in α-lamellas, whose size (thickness) is an order of magnitude less than that of α-globules. By substituting these values into Eq. (3) we obtain $\sigma_{-1}^{calc} = 1621$ MPa, which exceeds $\sigma_{-1}^{exp} = 800$ MPa by more than twice (Table 2).

Due to the discrepancy between the experimental and calculated results, the assumption can be made that the proposed formula (3) is incorrect. Although it can be considered that this size of the microstructural element, i.e., the thickness of the α-lamella, is not the very parameter on which the fatigue limit for the given material is dependent. The thickness of the colony of identically located lamellas (e.g., of 4 lamellas) can serve as this parameter since the slip planes within one colony have the same direction. However, this kind of assumption is likely to be wrong, because the α-lamellas that are located in some colony of the β-grain or randomly distributed in the grain, have their own boundaries with β-spacings between them, which (both the former and the latter) are the effective barriers to crack propagation. Moreover, as shown by the microstructure analysis, the colony of identically located α-lamellas can occupy the half or more of the β-grain ranging from 50 to 60 μm in size. That was why, when investigating the influence of the grain size on the fatigue limit, many researchers came to a deadlock explaining this "noninfluence" by other factors.

Instead, it is evident that with the grain subsequently becoming finer (for $d \to 0$), the fatigue limit cannot reach infinity but asymptotically approaches a certain constant value, i.e., the characteristic that is independent of the microstructure (or more specifically, of the grain size). As shown by the results of static tensile tests (stress-strain curves) of VT3-1 alloy [10], the proportionality limit, σ_p, can be served as this constant value. The values of $\sigma_p \approx 840$ MPa for all seven investigated structural states of this alloy. And this makes sense because all the fatigue limits for this alloy are below this value. Substitute the obtained value of σ_p for σ_{-1} into Eq. (3) and determine the so-called "minimum grain size," $d_{\min}$, below which the equation will not be valid. For VT3-1 alloy, we have $d_{\min}$ = 1.5 μm.

The fact is also evident that the lower bound of the fatigue limit exists for every alloy, since if $d \to \infty$, the fatigue limit cannot tend to zero but, instead, will approach a certain constant value that is independent of the grain size, namely, the value of the so-called "internal friction stress" in the grain, i.e., the stress required for dislocation movement in the crystal (an individual element of the structure). The internal friction stress, σ_f, can be calculated according to the Schmid law by the following formulas:

$$\sigma_f = 2\tau_c, \tag{6}$$

$$\tau_c = \frac{2G}{k'} e^{-2\pi a/(k'b)}, \tag{7}$$

where τ_c is the critical shear stress in the crystal lattice, $k' = 1$ is the coefficient for a screw dislocation, $k' = 1 - \mu$ for an edge dislocation, μ is Poisson's ratio, G is the shear modulus, and a and b are the parameters of the crystalline lattice. For simplicity, τ_c can be defined by the approximate formula [13]:

$$\tau_c \cong 10^{-3} G. \tag{8}$$

Substitute into Eq. (3) and determine the so-called "maximum grain size," $d_{\max}$, for which formula (3) can be used. For VT3-1 alloy $\{\mu = 0.3$ and $G = E/[2(1+\mu)] = 49$ GPa$\}$, we have $\sigma_f = 98$ MPa and $d_{\max} = 109$ μm.

Thus, the investigations and calculations performed for seven different microstructures of a two-phase titanium VT3-1 alloy allow us to come to the conclusion about the existence of some nonlinear relationship between the fatigue limit, σ_{-1}, of the material and the microstructure parameter, $1/\sqrt{d}$, that lies between the two asymptotes, $\sigma_{-1} = \sigma_f$ and $\sigma_{-1} = \sigma_p$. Taking this point into account and using it to approximate the function $\arctan(\cdot)$, we perform elementary mathematical transformations. As a result, we obtain the general grain-size dependence of the fatigue limit in the following form:

$$\sigma_{-1} = A + B \arctan \frac{C - A}{B}, \tag{9}$$

where

$$A = \frac{\sigma_f + \sigma_p}{2}, \qquad B = \frac{\sigma_p - \sigma_f}{\pi}, \qquad C = \frac{\Delta K_{th\,eff}}{Y\sqrt{d}}.$$

TABLE 3. Comparison of the Calculated σ_{-1}^{calc} and Experimental σ_{-1}^{exp} Results Obtained for VT3-1 Alloy

Microstructure No.	d, μm	σ_{-1}^{exp}, MPa	By formula (3)		By formula (9)	
			σ_{-1}^{calc}, MPa	Δ, %	σ_{-1}^{calc}, MPa	Δ, %
1	0.4	800	1621.0	+103.0	792.2	−0.97
2	1.8	750	764.0	+1.9	676.4	−9.80
3	2.0	700	725.0	+3.5	664.0	−5.10
4	2.5	650	649.0	−0.2	623.0	−4.10
5	3.0	600	592.5	−1.3	583.0	−2.80
6	4.0	520	512.6	−1.4	512.2	−1.50
7	10.0	350	324.2	−7.4	343.2	−1.90

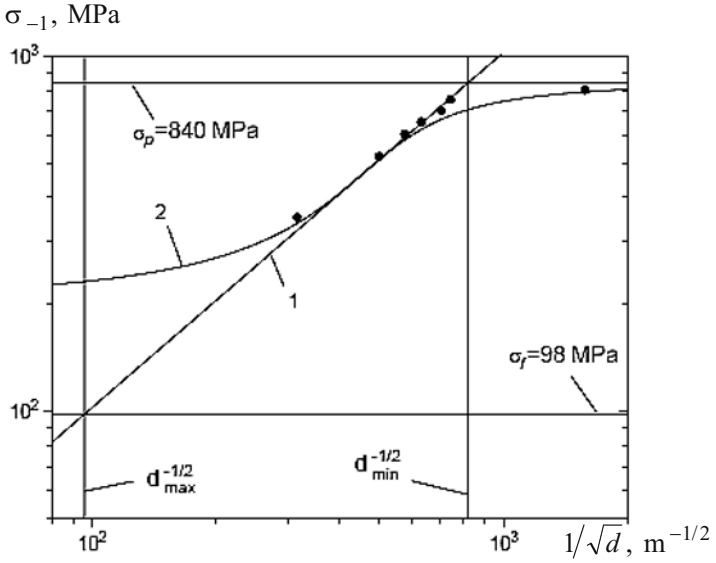

Fig. 3. Experimental dependence (points) and the dependences of the fatigue limit σ_{-1} on the average linear size d of the microstructural element of VT3-1 alloy calculated by formula 3 (*1*) and 9 (*2*).

The plot of the obtained dependence (9), curve *2*, in log–log coordinates is shown in Fig. 3 in comparison with the experimental results (points) for VT3-1 alloy. For comparison purposes, the figure also shows the plot of Eq. (3) (curve *1*). Table 3 presents the values of σ_{-1}^{calc} calculated by formula (9), which are indicative of satisfactory prediction of the results. The data given in Table 3 are represented graphically in Fig. 4 where the straight line $\sigma_{-1}^{exp} = \sigma_{-1}^{calc}$ shows perfect agreement between the experimental and calculated results.

Such nonlinearity of the dependence of σ_{-1} on $1/\sqrt{d}$ lies in the dual nature of the propagation of the microstructurally short and physically small fatigue cracks. Here, it is necessary to clarify the notion of the "microstructurally short" and "physically small" crack. According to Miller's classification [14], a flat shear crack of the depth $l \le d$ (grain size) should be considered as the microstructurally short one, whereas a three-dimensional crack of the depth $l < 10d$, but greater than d, that propagates both in shear (modes II and III) and in tension (mode I) should be considered as the physically small crack. A crack of the depth l_0 that corresponds to the fatigue limit will be considered as the physically small since its depth is within the above range.

On the one hand, the process of propagation and arrest of the crack at the level of the fatigue limit is governed by the effect of fatigue crack closure (FCC), according to which, as its length increases, the effective applied SIF range decreases to its threshold value. On the other hand, the tensile force necessary for nucleation and growth of a microstructurally short fatigue crack is due to both the external load (the external tensile force defined by the effective applied stress intensity factor range ΔK) and the elastic energy released by the local volume in the

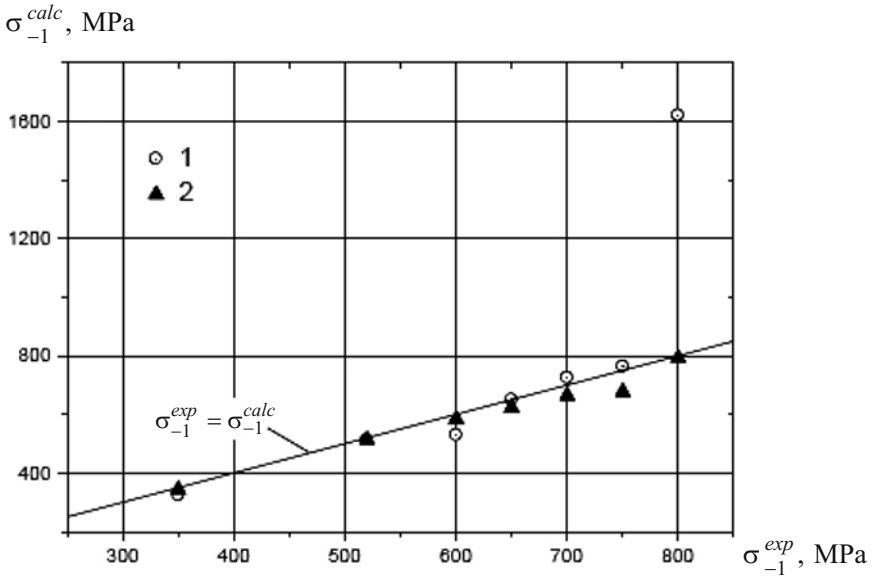

Fig. 4. Comparison between the results calculated by formulas (3) – (*1*) and (9) – (*2*) and the experimental ones for VT3-1 alloy.

vicinity of the crack tip, i.e., by the local tensile force. The initially high local tensile force value drops sharply if the energy accumulated in the small area of internal stresses is released due to the crack propagation. Instead, the external tensile force ΔK increases with the crack growth.

Moreover, the contribution to the local tensile force is made by the so-called "surface strain concentration phenomenon" [15]. That is, favourably oriented grains undergo the greatest surface deformation and, thus, the highest degree of the localized slip. The latter allows the development in favourably oriented grains of persistent slip bands, which later will be the most favourable nucleation site of a fatigue crack. Instead, grains of internal layers of the material "support" one another, resulting in the decrease in local strains with the movement into the specimen depth, which finally reach the nominal range.

Thus, as the size d of the structural element (grain) decreases, the value of l_0 which is a characteristic length (depth) of the crack defined by the fatigue limit σ_{-1} and threshold SIF, K_{th}, decreases too. Thus, previously [8] it was found that for a two-phase titanium VT3-1 alloy, with the sizes of the structural element responsible for the fatigue strength being $d_{7\alpha} = 10$ μm (a globular microstructure) and $d_{1\alpha} = 0.4$ μm (a lamellar microstructure), the value of l_0 (1) was equal to 64 and 2.2 μm, respectively (see Table 1, where numbers 1 and 7 correspond to the numbers of the microstructures). For all the microstructural states under study, the experimental values of σ_{-1} reached 350 and 800 MPa, K_{th} were 5.06 and 2.37 MPa$\sqrt{\text{m}}$, respectively, and the effective SIF range $\Delta K_{th\,eff}$ was 2.055 MPa$\sqrt{\text{m}}$ (in total, there were seven microstructural states, with two extremes in the size d being selected in this case for the purpose of contrast). It is evident that for a fine lamellar microstructure, the threshold SIF approaches the effective one. Thus, it can be concluded that the contribution of the fatigue crack closure effect is negligible, and the mechanism of fatigue crack propagation and arrest is mainly caused by the above process of redistribution of the local stresses, i.e., with the increasing length (depth) of such crack, the local stress drops, whereas the external (nominal) one increases. But owing to the fact that the crack is very small in this case, the process of reducing local stresses occurs more intensely than the process of increasing external tensile force, and the crack arrests.

The process of arrest of physically small cracks (of relatively small sizes for the specific material) can be interpreted another way. As is shown in [4], the process of FCC is characterized by a combined action of several mechanisms, the main of which are as follows: 1) the closure of a fatigue crack is due to the occurrence of a plastically deformed material at its faces; 2) the closure of a fatigue crack is due to the roughness of its faces; and 3) the closure of a fatigue crack is due to the formation of an oxide layer at its faces whose thickness is dependent on both the corrosion in the ambient environment and, to a great extent, on the fretting corrosion of the crack faces.

Therefore, it is logical to assume that as the grain size of the material decreases, the fatigue crack occurring at the fatigue limit level undergoes the effect of closure mainly through the mechanism of plastic deformation of the faces since the influence of other mechanisms decreases due to the reduction of the face roughness, and thus, the formation of a lesser number of fretting corrosion products, which, in its turn, results in the occurrence of an oxide film.

In any case, for different grain sizes ($d > d_{\min}$ and $d < d_{\min}$), the material behavior at the fatigue limit depends on different mechanisms of resistance to fatigue fracture. Namely, in the former case, it is the mechanism of fatigue crack closure, whereas in the latter case, it is the mechanism of the redistribution of local stresses i.e., the decrease in their range to the nominal value.

In a similar way, it is possible to explain the kink on the σ_{-1} versus $1/\sqrt{d}$ curve when σ_{-1} approaches the internal friction stress, σ_f, in the grain. In this case, the fatigue strength of the alloy will depend to a greater extent on the internal friction stress and the crystallographic texture than on the mechanism of fatigue crack closure. Thus, in the material with the grain size $d \approx d_{\min}$, the fatigue crack that has initiated at the fatigue limit level either should not exceed the grain size (i.e., it should be arrested near the first barrier) or should not initiate in the case of very large grains, since its occurrence will inevitably lead to fracture with the crystallographic texture favorable for this purpose. Thus, we have the third, grain size-dependent mechanism of the resistance to fatigue fracture that governs the material behavior at the level of the fatigue limit.

The grain-size (d) dependence of the fatigue limit σ_{-1} can also be represented in another way. As was indicated above, there is a proportional relationship between l_0 and d (2), where η is the coefficient of proportionality which, on the one hand, should be equal to the number of grains from the specimen surface to the crack tip, and on the other hand, as was shown in [8], it can be calculated in the following way:

$$\eta = \frac{1}{U^2}, \tag{10}$$

$$U = \Delta K_{th\,eff} / K_{th}, \tag{11}$$

where U is the coefficient of crack opening. So, it is reasonable to consider η as the coefficient of fatigue crack closure.

It should be reminded that, as was indicated above, $\Delta K_{th\,eff}$ is calculated by formula (4). In particular, it was indicated in [11] that for titanium alloys with a mean elastic modulus, $E \cong 1.16 \cdot 10^5$ MPa, $\Delta K_{th\,eff} / E \cong 1.8 \cdot 10^{-5} \sqrt{\text{m}}$. It is easy to see that the coefficient of proportionality in formula (4) is approximately equal to $\sqrt{a}$ where a is the crystal lattice parameter (interatomic distance); for pure α-titanium, $a = 2.95 \cdot 10^{-10}$ m [16]. In particular, the content of Al impurities (in atomic per cent) in titanium alloys from 0 to 12 reduces the interatomic distance a from $2.95 \cdot 10^{-10}$ to $2.93 \cdot 10^{-10}$ m. Since the content of Al in different titanium alloys varies approximately from 0 to 6.6%, the maximum error in the calculations of $\sqrt{a}$ does not exceed 0.6 %. Therefore, in what follows, the variations in the content of impurities were neglected for simplicity, and the values of a for pure α-titanium were included in the calculation. Then, formula (3) can be written in the following way:

$$\sigma_{-1} = \frac{E}{Y}\sqrt{\frac{a}{d}} \cong E\sqrt{\frac{a}{4d}} = E\sqrt{\frac{a}{\eta d}}. \tag{12}$$

By analogy with formula (3), Eq. (12) is valid in a certain range of grain sizes, as was described above. Similarly to formula (9), the following relationship is valid for any grain size:

$$\sigma_{-1} = E\sqrt{\frac{a}{\eta' d}}, \tag{13}$$

TABLE 4. Comparison between the Calculated and Experimental Results

No. of the microstructure	σ_{-1}^{exp}, MPa	By formula (3)		By formula (9)		By formula (12)		By formula (13)	
		σ_{-1}^{calc}, MPa	Δ, %	σ_{-1}^{calc}, MPa	Δ, %	σ_{-1}^{calc}, MPa	Δ, %	σ_{-1}^{calc}, MPa	Δ, %
1	800	1621.0	+103.0	792.2	−0.97	1731.0	+116.0	796	−0.5
2	750	764.0	+1.9	676.4	−9.80	816.0	+8.8	699	−6.8
3	700	725.0	+3.6	664.0	−5.10	774.0	+10.6	685	−2.2
4	650	649.0	−0.2	623.0	−4.10	692.5	+6.6	648	−0,3
5	600	592.5	−1.3	583.0	−2.80	632.0	+5.3	612	+2,0
6	520	512.6	−1.4	512.2	−1.50	547,5	+5.1	545	+4,8
7	350	324.2	−7.4	343.2	−1.90	346.0	−1.1	356	+1,7

where

$$\eta' = \frac{E^2 a}{d} \Bigg/ \left[A + B \arctan\left(\frac{E\sqrt{a/(\eta d)} - A}{B} \right) \right]^2 , \tag{14}$$

with the quantities A and B being the same as in Eq. (9).

Thus, the parameter η' determines the number of barriers before fatigue crack arrest at the fatigue limit level by taking into consideration which grain size-dependent mechanism of the resistance to propagation of a physically small crack governs the material behavior.

Noteworthy is the following finding. If formula (14) is used for VT3-1 alloy (Table 1, $d = 0.4$ μm), we obtain $\eta' = 18.7$. By substituting the values obtained experimentally for σ_{-1} and K_{th} [8] into Eqs. (1) and (2), we get

$$l_0 = \frac{K_{th}^2}{\sigma_{-1}^2 Y^2} = \frac{(2.37)^2}{(800)^2 (1.99)^2} \cong 2.2 \text{ μm}, \qquad \eta = 2.2/0.4 = 5.5.$$

The number of grains (barriers) that are overcome by the crack before its arrest increases with a decrease in their sizes, and vice versa, it decreases with an increase in grain sizes (Fig. 3). This means that formula (1) cannot be used for both “very small grains” and “very great ones” for one specific material.

It is also logical to assume that if Y is the so-called geometric function for long cracks, then $\sqrt{\eta'}$ in formula (13) is the geometric function for physically small cracks.

Table 4 presents the results calculated by formulas (12) and (13) and previous calculations by formulas (3) and (9) in comparison with the experimental results that show a very good agreement for the cases of formulas (13) and (9).

Instead, the advantage of formula (13) over formula (9) is in the availability of the parameter $\eta' = f(d)$ that defines the number of barriers before the fatigue crack arrest at the fatigue limit level depending on the material grain size.

In order to establish the fact that the proposed models for the fatigue limit are general, i.e., valid for various classes of materials, the grain size-dependent experimental data for fatigue limits σ_{-1} were found in the literature for alloys with another type of the crystal lattice, namely, the fcc (brass of composition 70% Cu/30% Zn [17–20]) and the bcc lattice (steel with 0.16% C [5, 7, 20–22]). For the majority of metals, the value of the proportionality limit σ_p is close to that of the apparent elastic limit $\sigma_{0.001(0.003-0.01)}$ [22]. The limitation of σ_p as a calculated quantity is the absence of normalized values for structural metals and alloys. In the majority of current standards and specifications, this parameter is absent. Therefore, if there is a need to use this value for the calculation purposes, it is necessary to perform either special experiments to define it, or to be satisfied with the values for individual melts of this alloy given in the literature. In contrast to titanium alloys having a hexagonal close-packed (hcp) α-lattice that

TABLE 5. Comparison between the Calculated and Experimental Results

Material	$E\cdot10^{-5}$, MPa	By formulas (6) and (8) σ_f, MPa	σ_p, MPa	d, μm	σ_{-1}^{exp}, MPa	By formulas (3)		By formulas (9)	
						σ_{-1}^{calc}, MPa	Δ, %	σ_{-1}^{calc}, MPa	Δ, %
Steel 0.16% C [20, 21]	2	162	270 [5]	31	230.0	289.0	+25.5	255.0	+10.80
				45	200.0	240.0	+20.0	237.0	+18.00
				100	180.0	161.0	−10.5	181.0	+0.60
				104	180.0	158.0	−12.4	180.3	+0.16
				170	175.0	123.0	−29.5	174.2	−0.50
				198	175.0	114.0	−34.7	174.7	−1.00
Brass 70/30 [17–19]	1	70	120 [22]	18	142.0	189.0	+33.0	118.0	−17,00
				22	123.0	171.0	+39.0	117.0	−4.90
				33	110.0	140.0	+27.0	115.0	+4.50
				40	104.0	127.0	+22.0	113.0	+8.40
				51	98.5	112.0	+14.0	108.0	+9.60
				75	94.0	93.0	−1.0	93.0	−1.00
				131	84.5	70.3	−16.8	79,0	−6.50
				330	80.0	44.3	−44.6	75.0	−6.00
				330	69.0	44.3	−35.8	75.0	+8.70

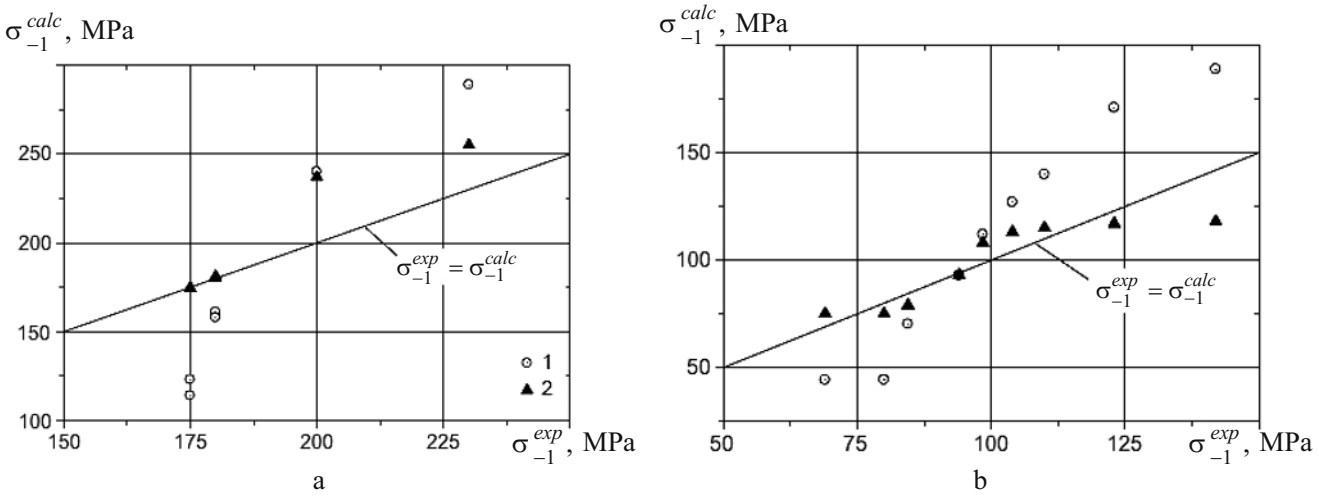

Fig. 5. Comparison between the calculated and experimental results for steel (0.16% C) (a) and for brass 70/30 (b) by formula (3) – (*1*) and by formula (9) – (*2*).

are cyclically stable at low stress amplitude levels close to the fatigue limit or such that are softened at high stress amplitude levels [16], brass 70/30 is the material that is hardened under cyclic loading, i.e., the proportionality limit can increase, whereas a steel containing 0.16% C is the softened material, the proportionality limit can decrease [4]. Therefore, since the data for σ_{-1} were selected from different sources, the values of the proportionality limit were selected for the calculation in the following way: $\sigma_{p\max} = 270$ MPa for a steel containing 0.16% C [5], and $\sigma_{p\min} = 120$ MPa for brass 70/30 [21]. That is, the maximum value of σ_p was selected for the softening material, and the minimum one – for the hardening case.

Table 5 presents the results for grain size d-dependent calculations of σ_{-1}^{calc} made by formulas (3) and (9). As seen, the calculation by formula (9) gives a satisfactory result for both of the selected materials, in contrast to that by formula (3) which yields a considerable error. Thus, Δ is in the range from +25.5% to –34.7% for steel containing 0.16% C and in the range from +39% to –44.6% for brass 70/30. The comparison results between the calculated and experimental data (Table 5) are shown in Fig. 5.

The results obtained are indicative that formula (9) can be used as the universal grain-size d dependence of the fatigue limit σ_{-1} of the material, i.e., it is valid for materials with different types of crystal lattice, but certainly with regard to the above constraints.

The calculation by formulas (12) and (13) could not be performed, since no values of the interatomic distance a were available for these alloys in the literature.

CONCLUSIONS

1. Using a two-phase titanium VT3-1 alloy with a different microstructure as an example, it has been shown that the dependence of the fatigue limit σ_{-1} on the structural parameter $1/\sqrt{d}$ has a nonlinear nature.

2. The generalized model (9) and (13) developed for calculating the fatigue limit has shown very good agreement with the experimental results [$\Delta_{(9)} = (-1)$–(-9.8%) and $\Delta_{(13)} = (-0.3)$–$(+4.8\%)$].

3. It has been found that the structural parameter responsible for the fatigue strength of the material under study is the linear size (diameter) of α-globules for bimodal and globular microstructures and the thickness of α-lamellas for a lamellar microstructure.

4. The calculation of σ_{-1} by the proposed model (9) for alloys with different type of crystal lattice [steel containing 0.16% C (bcc) and brass 70/30 (fcc)] is indicative of the satisfactory result as compared to the experimental one, in contrast to the calculation by formula (3), which has a significant error [(+30)–(−44.6%)]. This is indicative that the model (9) is valid for materials with different types of crystal lattices.

REFERENCES

1. E. O. Hall, "The deformation and ageing of mild steel. III. Discussion of results," *Proc. Phys. Soc. London*, **B64**, 747–753 (1951).
2. A. Cracknell and N. J. Patch, "Frictional forces on dislocation at lower yield point in iron," *Acta Met*., **3**, 186–189 (1955).
3. R. W. Armstrong, "The influence of polycrystal grain size on several mechanical properties of materials," *Metall. Trans*., **1**, 1169–1176 (1970).
4. V. V. Panasyuk (Ed.), *Fracture Mechanics and Strength of Materials*, Handbook in 4 volumes, Vol. 4: O. N. Romaniv, S. Ya. Yarema, and G. N. Nikiforchin (Eds.), *Fatigue and Cyclic Fracture Toughness of Structural Materials* [in Russian], Naukova Dumka, Kiev (1990).
5. V. T. Troshchenko (Ed.), *Material Resistance to Deformation and Fracture* [in Russian], Handbook in 2 volumes, Naukova Dumka, Kiev (1993).
6. M. M. El Haddad, K. N. Smith, and T. U. Topper, "Fatigue crack propagation of short cracks," *Trans. ASME*, *J. Eng. Mater. Technol*., **101**, No. 1, 42–46 (1979).
7. V. T. Troshchenko, B. A. Gryaznov, Yu. S. Nalimov, et al., "Fatigue strength and cyclic crack resistance of titanium alloy VT3-1 in different structural states. Communication 1. Study procedure and experimental results," *Strength Mater*., **27**, No. 5-6, 245–251 (1995).
8. O. N. Herasimchuk, *Endurance and Cyclic Crack Growth Resistance of Titanium Alloy VT3-1 in Different Structural States* [in Russian], Author's Abstract of the Candidate Degree Thesis (Tech. Sci.), Kiev (1995).
9. V. N. Gridnev, O. M. Ivasishin, and S. P. Oshkaderov, *Physical Foundations for High-Speed Thermal Hardening of Titanium Alloys* [in Russian], Naukova Dumka, Kiev (1986).
10. *Mechanical Properties of a Titanium Blading Alloy*, CS-2933. Final Report EPRI Research Project (Oct. 1983).
11. P. K. Liaw, T. R. Leax, and W. A. Logston, "Near-threshold fatigue crack growth behaviour in metals," *Acta Met.*, **31**, No. 10, 1581–1587 (1983).
12. *RD 50-345-82. Strength Analysis and Tests. Methods for Mechanical Testing of Metals. Determination of Fracture Toughness Characteristics under Cyclic Loading (Methodological Recommendations)* [in Russian], Izd. Standartov, Moscow (1983).

13. A. Ya. Krasovskii, *Physical Foundations for Strength* [in Russian], Naukova Dumka, Kiev (1977).
14. K. J. Miller, "The two thresholds of fatigue behaviour," *Fatigue Fract. Eng. Mater. Struct.*, **16**, No. 9, 931–939 (1993).
15. H. Abdel-Raouf, D. L. DuQuesnay, T. H. Topper, and A. Plumtree, "Notch-size effects in fatigue based on surface strain redistribution and crack closure," *Int. J. Fatigue*, **14**, No. 1, 57–62 (1992).
16. G. Lutjering and J. C. Williams, *Titanium*, Springer Verlag, Berlin; Heidelberg (2003).
17. V. S. Ivanova and V. F. Terent'ev, *Nature of the Fatigue of Metals* [in Russian], Metalluguiya, Moscow (1975).
18. G. M. Sinclair and W. J. Craig, "Influence of grain size on work hardening and fatigue characteristics of alpha brass," *Trans. ASM*, **44**, 929–940 (1952).
19. P. G. Forest and A. E. L. Tate, "The influence of grain size on the fatigue behaviour of 70/30 brass," *J. Inst. Metals*, **93**, 438–444 (1965).
20. V. F. Terent'ev and V. G. Poida, *Fatigue and Fracture Toughness of Metals* [in Russian], Nauka, Moscow, (1974), pp. 109–140.
21. T. Ekobori, *Physics and Mechanics of Fracture and Strength of Solids* [Russian translation], Metallurgiya, Moscow (1971).
22. P. B. Mikhailov-Mikheev, *Handbook on Metallic Materials in Turbine and Engine Construction* [in Russian], Mashgiz, Moscow (1961).